Powder Technology 395 (2022) 280–289

Contents lists available at ScienceDirect

Powder Technology

journal homepage: www.elsevier.com/locate/powtec

Freeze granulation and spray drying of mixed granules of Al_2O_3

M. Singlard [a,b], A. Paillassa [a], L. Ferres [a], C. Pagnoux [b], A. Aimable [b,*]

[a] Institut de Recherche Technologique Saint Exupéry, Esplanade des arts et métiers, 33405 Talence, France
[b] Univ. Limoges, CNRS, IRCER, UMR 7315, F-87000 Limoges, France

ARTICLE INFO

Article history:
Received 30 June 2021
Received in revised form 15 September 2021
Accepted 16 September 2021
Available online 22 September 2021

Keywords:
Spray drying
Freeze granulation
Alumina
Size distribution
Binder
Granules

ABSTRACT

This paper proposes a comparative study of two techniques of granulation of a submicronic alumina powder with high binder content slurries, by spray drying and freeze granulation for the preparation of mixed granules. First, the viscosity and flow index of the suspensions are given as a function of dispersant, solid and binder contents versus alumina content, and the data are analysed in order to give a predictive model in a wide range. Suspensions with varying viscosities (7–208 mPa.s), densities (1.31–1.76) and surface tensions (23–40 mN/m) were then granulated. The first observations reveal the importance of the content and the molar mass of the binder: when they are too high, the freeze granulation fails and filaments are produced instead of granules due to extensive stretching of the molecular chains of the binder during spraying. Then through a theoretical analysis of the phenomena leading to granulation, an original dimensionless number is proposed to describe the evolution of the granule size as a function of suspension formulation. This number is related to the Reynolds and Weber number and is able to predict the granule size over a wide range (20–500 μm for freeze granulation, and 5–30 μm for spray drying). Spray drying leads to smaller granules with various shapes, from full shape to hollow or donut-like, whereas freeze granulation leads to bigger but spherical granules with a microporosity, and a size easier to predict as no drying shrinkage is observed.

1. Introduction

Granulation techniques are widely used in many industrial sectors, and for various purposes. The pharmaceutical industry uses granulation for coating or encapsulation of active ingredients [1]. In the food industry, granulation provides additional properties such as aesthetic, shelf life, odor, taste, UV or moisture protection etc. In the ceramic industry, granulation is used to facilitate the flow of powders, and therefore their handling by dosers and conveyors. It also improves the pressability of the materials, and thus green density and densification rate for sintering. Another application is for the preparation of intimate ceramic-organic mixtures for specific processes such as Selective Laser Sintering [2–4]. Granulation techniques can also be used to improve bulk density and fluidity of nanoscale powders to increase their workability while maintaining their other properties as required to build nanostructured coating by plasma spraying [5,6]. In all these application, a good control of the granule size and morphology is required, as it impacts the green mechanical properties of the granules [7].

The spray drying process consists of pumping a suspension or a solution to a spray nozzle, then drying the resulting droplets in a chamber containing a stream of hot gas (usually air but could be nitrogen for oxidation-sensitive materials) and finally collecting with a cyclone (or other technique) the dry granules formed [1]. Depending on the way in which the suspension is atomized into fine droplets, a distinction is made between pressure nozzle atomizers, rotary atomizers and pneumatic atomizers [8]. The gas flow can be in the same direction as the spray (so-called co-current atomization) or in the opposite direction (so-called counter-current atomization). The shear rates experienced by the suspension during spraying can reach values as high as 10^6 s^{-1} [9]. To encapsulate a ceramic powder in a polymer, spray drying can be used as it has been the case with alumina, glass or silicon carbide powders [2–4,10]. The granule size increases with the suspension viscosity [9], solid content [11,12], surface tension [1], particle size [13], feed rate [1] and nozzle diameter [1]. It decreases with the density of spraying gas, atomization pressure [1] and, for rotary atomizers, with rotational speed and diameter of the rotating disc [8]. During the drying of the granules (after spraying), the species in solution tend to migrate with the liquid to the surface. This phenomenon leads to segregation of the species in solution, most of which are then found on the surface. Typically, this occurs when using suspensions with organic additives, such as binders. Although the binders have a certain affinity with the oxide surfaces, a large part of them is found in solution. For example, Baklouti et al. determined that the adsorption limit of polyvinyl alcohol (PVA) on the alumina surface is around 0.6 mg/m^2 [14]. Therefore,

* Corresponding author.
E-mail address: anne.aimable@unilim.fr (A. Aimable).

https://doi.org/10.1016/j.powtec.2021.09.044
0032-5910/

Nomenclature

Latin letters

C	Volume percent of dry matter in the suspension
$C^{vol}_{alumina}$	Volume percent of alumina in the suspension
C^{vol}_{add}	Volume percent of organic additive in the suspension
d	Drop diameter (m)
d_{50}	Mean diameter by volume (m)
d_n	Nozzle diameter (m)
K	Constant in Herschel-Bulkley model
Mat	Part of Pu′ related to material properties
n	Flow index
Pro	Part of Pu′ related to process properties
P_s	Spraying stress (Pa)
Pu	Pulverization number
Pu′	Modified pulverization number
P_γ	Stress related to surface tension (Pa)
P_η	Viscous stress (Pa)
R	Volume percent of organic additive on the total dry matter
Re*	Modified Reynolds number
u	Gas velocity (m/s)
We*	Modifier Weber's number
X	Dispersant content relative to alumina surface (kg/m^2)

Greek letters

β_1	Fitting constant in the expression of Pu′
β_2	Fitting constant in the expression of Pu′
$\dot{\gamma}$	Shear rate (s^{-1})
η	Dynamic viscosity (Pa.s)
ρ	Density (kg/m^3)
τ	Shear stress (Pa)
τ_0	Yield stress (Pa)

when the amount is higher, the binder remains in solution and migrates to the surface of the droplets during drying. Binder segregation is promoted by a high binder content, a large amount of liquid, large granule and drop sizes, and a high solvent evaporation rate [15].

Freeze-granulation consists in spraying a suspension above a bath at very low temperature (usually liquid nitrogen) to freeze the droplets before they dry [16]. The extremely fast cooling rate allows the solvent (usually water) to solidify without crystallization. The frozen granules are then recovered and dried by lyophilization, i.e. liquid sublimation. Since the spraying method of the freeze granulation is the same as these by atomization, all spraying parameters affecting the granules size are identical [17]. Granule density increases with solid content. Granule surface is smoother when the solid content of the suspension is higher. Freeze granulation can overpass the quality of spray drying when the product is sensitive to high temperature. In addition, due to fast freezing and lyophilisation, the granules are mainly spherical, contrary to spray drying [18]. Although more complex to implement, freeze granulation may be preferred to spray drying when the product to be treated is very sensitive to the high temperatures required for drying. In addition, it can be complex to obtain full and spherical granules by spray drying because of the migration phenomenon mentioned above, whereas freeze granulation ensures spherical, homogeneous and low density granules that is useful for dry pressing operation to achieve high green density (better pressability thanks to low granule density), high green strength (strength of a non-sintered ceramic) and better homogeneity [19]. When high homogeneity granules (multi-material granules) are required, as for nuclear applications [20] and transparent ceramics [21], freeze granulation is recommended. Freeze granulation could be useful for 3D printing techniques which used powder bed like binder jetting [22,23]. In addition, for hazardous powders, freeze granulation is a better option than spray drying because it is a dust-free process [24].

These previous studies have revealed the importance of some experimental parameters and their influence on the final granule size and their morphology. However, only trends are derived from these studies (size increases or decreases with a given parameter) and it is not possible to determine in advance the size of a granule using the characteristics of the suspension and the granulation process. In this paper we propose a new parameter called Pu (for pulverization number), able to predict the granule size through a multi-parameter approach, taking into account both slurry and process parameters. This study was conducted in the context of the formulation of mixed granules of alumina with a high content of organic binders to improve their plasticity at a medium temperature. Thus in a preliminary study the rheological behaviour of the suspensions was conducted to optimize their formulations and better predict the influence of the relative concentrations of dispersant and binder to the alumina content.

2. Materials and methods

2.1. Materials

Alumina powder is supplied by Alteo, France, under the reference P172LSB. Specific surface area is measured at 8.6 m^2/g (BET method) and the mean diameter at 0.4 μm (laser diffraction method). According to the supplier, the alumina content is 99.8%.

The dispersant used is an ammonium polymethacrylate (Darvan C-N, Vanderbilt) with molar mass of 10–16 kg/mol.

Three organic additives of different molecular weight are used: polyethylene glycol (from 4 to 100 kg/mol, named PEG-1 to PEG-3), polyethyloxazoline (from 50 to 500 kg/mol, named PEOx-1 to PEOx-5), and a rosin ester (RE). PEG and PEOx are water soluble in large proportion whereas RE is modified with a surfactant to make it dispersible in water.

The surface tension of the suspension is controlled thank to 0.04 v.%. of a polyether-modified siloxane surfactant (BYK348, BYK Chemie).

2.2. Formulation of the suspensions and procedure for their preparation

Different formulations of suspensions were prepared by varying the concentration of the dispersant (X), the content of the organic additives (R) and the solid content (C), as defined below:

- **X is the dispersant content (mass of dispersant/surface of alumina), in mg/m^2.** Since the dispersant adsorbs on the ceramic particles surface, the dispersant content in mg/m^2 is better suited than in wt%.
- **R is the volume percent of organic additive on the total dry matter** (organic additives + alumina) $R = \frac{C^{vol}_{add}}{C^{vol}_{add}+C^{vol}_{alumina}}$, in **vol%.** R is a key parameter, which represents the ratio of organic binder in the final granule.
- **C is the volume percent of dry matter in the suspension** ($C = \frac{C^{vol}_{add}+C^{vol}_{alumina}}{C^{vol}_{water}}$, in **vol%).**

The procedure for the preparation of these suspensions is as follows (also detailed in Supplementary Materials). The powder is added gradually in an aqueous solution of dispersant while stirring. The suspension is then deagglomerated by an ultrasonic treatment and then, placed for 15 h on rollers to allow dispersant adsorption on the powder surface. This suspension is referred to as the mother suspension. The additive (PEG or PEOx) is solubilized in water under agitation at room temperature prior to its introduction into the mother suspension to ensure a better homogeneity. The RE additive is already supplied as an aqueous dispersion by the manufacturer and is used as received. In the case of an additive mixture, the polymers are introduced in descending order

of molar mass, because the dissolution of the additives of high molecular weight is easier when the solution is less viscous. Once the additive solution is introduced into the mother suspension, the sample is stirred for 90 min and then the surfactant is introduced. After a further 90 min of homogenization, the surface tension and viscosity of the suspension are measured. Finally, the sample can be granulated, either by freeze granulation or spray drying.

2.3. Granulation of the suspensions: freeze granulation and spray drying

Freeze granulation (Fig. 1a) is carried out using a PowderPro apparatus equipped with an external mixing nozzle with a 1.4 mm opening. The suspension feed rate and the air velocity are set respectively at 36 mL/min, and from 87 to 204 m/s. The distance between the nozzle and the liquid nitrogen is about 20–30 mm. This distance is an order of magnitude greater than the calculated distance (using the ratio of the dynamic pressures of the fluid and air) of jet breakage under the experimental conditions used [25]. Granules are freeze-dried (Beta 2–8 LDplus, Christ) for 18 h.

The suspension is poured into one beaker and the liquid nitrogen into another. Both are kept under agitation by magnetic stirrers. A peristaltic pump drives the suspension into the nozzle. The nozzle is connected to compressed air, the pressure of which is adjusted in order to vary the air velocity at the nozzle outlet. The nozzle is mounted at the top of the beaker in its center. When the suspension beaker is empty, the airflow is stopped. A metal tray supplied with the freeze dryer is filled with liquid nitrogen until boiling stops, meaning that the tray has reached the temperature of liquid nitrogen. With a ladle, the frozen granules are collected and poured into the tray. During the transfer, the granules remain covered with liquid nitrogen to ensure that they remain frozen. Once all the frozen granules are recovered, the tray is inserted into the freeze dryer and the sublimation cycle begins. At the end of the cycle, the freeze-dried granules are collected in a vial for further analysis.

Spray drying (Fig. 1b) is carried out with two equipments named hereafter SD1 (Buchi Mini Spray Dryer, 190) and SD2 (Buchi Mini spray Dryer B-290). These equipments are lab-scale machines and are very similar in their principle and use. They are from different generation, working thanks to an internal mixing nozzle.The drying air flow is co-current and the dried granules are collected with a cyclone. The inlet temperature is set at 190–220 °C in order to achieve an outlet temperature (measured just before the cyclone) of 90–120 °C. In internal mixing nozzles, suspension and air are ejected through the same orifice. Thus, even knowing the air and suspension flow rates (in m^3/s), it is not possible to simply deduce the air velocity (in m/s) because the cross-sectional area (in m^2) is not equal to the nozzle diameter (due to the simultaneous passage of the suspension and air through this diameter). The air velocity is therefore not indicated, but the pressure in the air circuit is kept constant for all experiments.

2.4. Characterization techniques

The rheological properties of the suspensions are measured by a rheometer (ARG2, TA Instruments) with a cone-plate geometry (titanium, 60 mm, 2°) from 10 to 300 s^{-1} in shear rate at 20 °C. All the viscosity values presented in this article are taken at 100 s^{-1}.

The Wilhelmy method is used to measure the surface tension of the suspension (DCAT11, Dataphysics). The plate is made of platinum-iridium alloy. The Wilhelmy method assumes that the contact angle between the plate and the sample is (near) zero. The platinum-iridium alloy produces a zero contact angle with most liquids. To avoid pollution that could change the contact angle value, the plate is cleaned in the flame of a Bunsen burner before each measurement. The surface tension is measured continuously until the standard deviation of the last 50 points is below 0.03 mN/m. The surface tension measurement is the mean of these 50 points.

The size distribution of the granules is measured by laser diffraction (Mastersizer 2000, Malvern), using a dry route with a 1 bar pressure. For each sample, the powder is fed into the equipment continuously, and three measurements are averaged.

The morphology of the granules is observed by scanning electron microscopy (SEM, Jeol IT300 LV) with secondary electrons, a 5 kV accelerating voltage and 8–10 mm working distance. Before observation, samples are metallized by a 15 nm thick platinum layer.

3. Results and discussions

3.1. Rheological behaviour of the suspensions for the granulation process

Ceramic suspensions with organic additives exhibit generally a non-Newtonian behaviour which can be described by the Herschel-Bulkley law (Eq. 1).

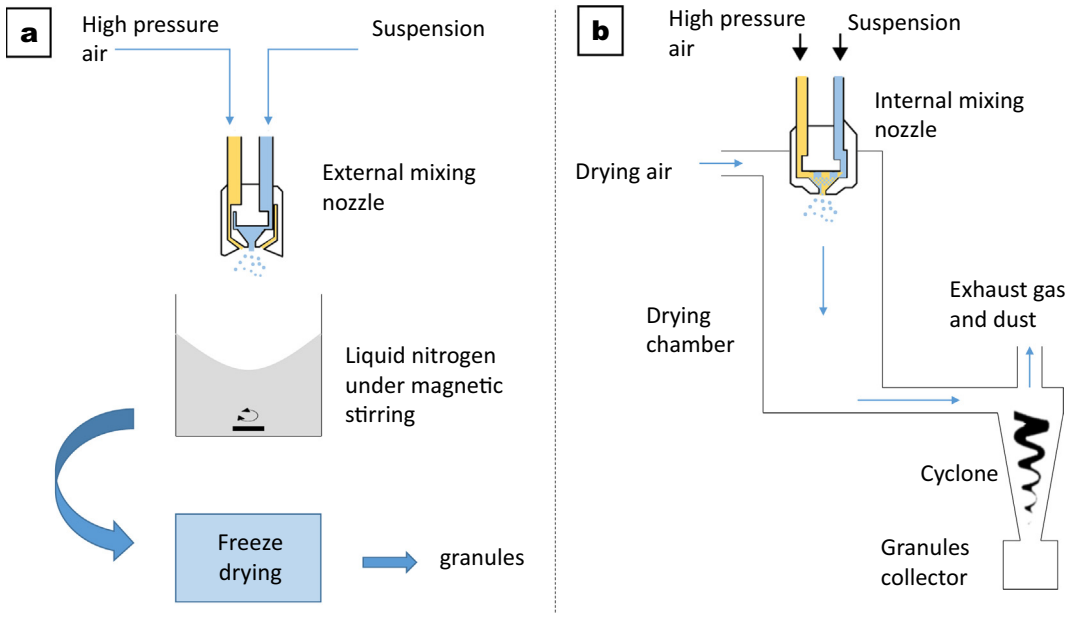

Fig. 1. Description of (a) freeze granulation and (b) spray drying processes.

$$\tau = \tau_0 + K\dot{\gamma}^n \quad (1)$$

Where τ is the shear stress (Pa), $\dot{\gamma}$ the shear rate (s^{-1}), τ_0 the yield stress (Pa), n the flow index and K a constant. The yield stress is the minimal shear stress required to initiate flow. The flow index represents the deviation from a Newtonian behavior: if $n < 1$, the suspension is shear thinning and if $n > 1$, the suspension is shear thickening.

Nine suspensions were formulated with the additive PEOx-5, by varying the concentration of dispersant X from 0.1 to 1.0 mg/m^2, the organic content R from 20 to 50 vol%, and the solid content C from 15 to 30 vol%. From these experiments, the variations of viscosity and flow index were modeled using polynomials of degree 2 (least squares fitting). All available polynomials, using any number of monomials (from 1 to 7) were calculated and, for each property (viscosity and flow index with each additive), the best polynomial was selected. All the selected models use only two of the three variables (X, R or C), which allows a representation in graphs where the two variables are arranged in abscissa and ordinate. A colour scale (blue for the lowest value and red for the highest) represents the value of the viscosity or the flow index. The isovalue curves are represented in black.

The viscosity and the flow index measured are reported in Fig. 2 (black dots) (details in table S1 in Supplementary materials). A model has been adjusted by the best polynomial of degree 2 (using the method of least squares). This model presents an adjusted R-square superior to 95%.

We can deduce from this model that the viscosity of the suspensions varies from 25 to 1000 mPa.s (Fig. 2a) and is not dependent on the dispersant content (X) in the measuring range (0.1 to 1.0 mg/m^2). Baklouti *et al.* [26] and Cesarano *et al.* [27] find that the adsorption of polymethacrylate onto the alumina surface is maximal around 0.36 mg/m^2 but it seems that the viscosity remains low also for higher or lower values. Otherwise, the higher the organic content on dry matter (R), and the solid content (C), the higher the suspension viscosity. When the organic fraction of dry matter is high (R large), the increase in viscosity with dry matter content is faster. If the dry matter is 26% organic ($R = 26\%$), the viscosity increases from 62 mPa.s to 146 mPa.s (+135% increase) when the dry matter/water ratio (i.e. C) increases from 21% to 30%. For $R = 44\%$, the viscosity increases from 168 to 628 mPa.s (+274% increase) over the same C range (20 to 30%). Therefore, the organic part of the suspension has a high impact on its viscosity.

The flow index of these suspensions ranges from 0.86 to 1 (Fig. 2b), which means that the suspensions containing PEOx5 are all shear thinning. The flow index is not affected by the dry matter concentration (C), and only by the composition of the dry matter (R) and the dispersant content (X). However, R has only a moderate impact on the flow index as shown by the quasi-vertical isovalue curves in the figure. The flow index evolution with dispersant concentration (X) is non-linear with a maximum for about 0.7 mg/m^2 (Fig. 2b), which corresponds to a newtonian behaviour ($n = 1$). This type of evolution has already been observed by Zhou *et al.* [28].

Nine suspensions were also formulated with the resin RE, by varying the concentration of dispersant X from 0.1 to 1.0 mg/m^2, the organic content R from 20 to 50 vol%, and the solid content C from 40 to 60 vol%. The viscosity and the flow index measured are reported in Fig. 3 (black dots) (details in table S1 in Supplementary materials), and a model adjusted in the same conditions.

The viscosity of the suspensions containing RE is much lower than the one measured with PEOx-5 in the whole range, as it varies from about 5 to 35 mPa.s (Fig. 3a). It depends mainly on the dry matter concentration (C) and the dispersant content (X), whereas it is not affected by the composition of the dry matter (R), which means that RE and alumina have the same impact on it. For a same dry matter concentration (C), a lower amount of dispersant produces a lower viscosity. Finally, the low viscosity values obtained (15 mPa.s for C = 40%) show that alumina dispersed with ammonium polymethacrylate and RE are highly compatible.

The flow index of the suspensions containing RE varies from 0.74 to 1.0 (Fig. 3b), corresponding to a shear thinning behaviour. Again, as for the viscosity, the composition of the dry matter (R) has no impact on this parameter. The higher the dispersant content (X) and the higher the dry matter content (C), the more shear thinning the suspensions are.

This preliminary study allows a good prediction of the rheological behaviour of the suspensions containing different organic additives. A wide range of concentrations could be explored through a simple polynomial modeling, combining the influence of organics concentration and the total solid content. This is an original and efficient approach to optimize the formulations for a given ceramic process in a liquid route such as granulation (freeze granulation and spray drying).

3.2. Suspension behaviour during freeze granulation

In the following, we make a focus on some limitations which are observed for the freeze-granulation of suspensions containing organics with the higher molecular weight (PEG-3). With 5 vol% of PEG-3, no

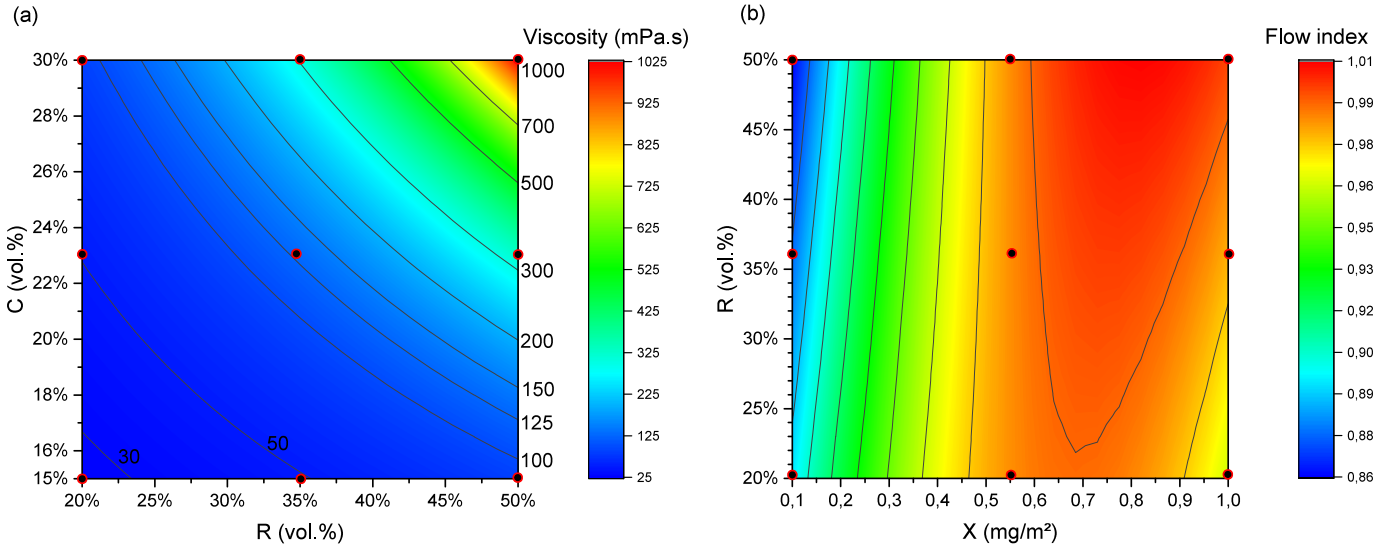

Fig. 2. (a) Viscosity and (b) flow index of the suspensions with PEOx-5 as organic additive. Black dots are the experimental data.

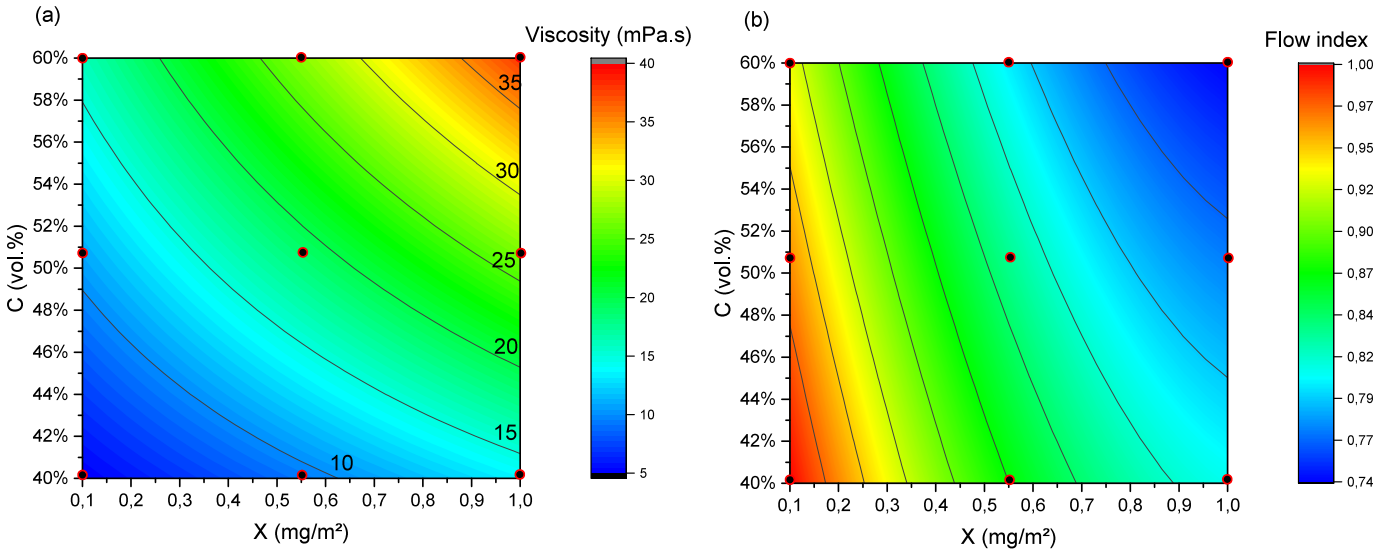

Fig. 3. (a) Viscosity and (b) flow index of the suspensions with RE as organic additive. Black dots are the experimental data.

granule is obtained and a large amount of thick filament are observed (Fig. 4a) whose diameter is measured at 25 μm (mean of 10 measurements). By reducing the solid content, some granules could be produced with a lower amount of thinner (11 μm) filaments (Fig. 4b). By reducing the polymer content and increasing the alumina content, thus conserving a close value for the viscosity (from Fig. 4c to d), spherical granules are obtained with a low content of filament.

Fig. 5 shows the granules obtained with suspensions at the same concentrations of alumina and polymer, but with PEG of different molecular masses. The filaments are only observed with the higher molecular mass (PEG-3), no filaments are produced for the two lower molar masses of PEG polymer (PEG-1 and PEG-2).

In the freeze granulation process, the liquid jet is pulverized by the high speed air. Due to the surface tension, each fragment forms spherical droplets, which become granules after freeze-drying. However, polymer solution jets have a different behaviour from Newtonian liquids due to the polymer chains elongation during stretching taking place during spraying. Depending on the formulation, several centimeters-long filaments can be produced. The formation and stability of these filaments have already been studied [29,30]. The filaments have a natural tendency to become thinner over time. Oliveira and McKinley have found that the decay in the filament radius (and therefore breakage when radius becomes equal to zero) is slower with higher molecular weight and polymer concentration [31]. Thus, if the molar mass and concentration of the

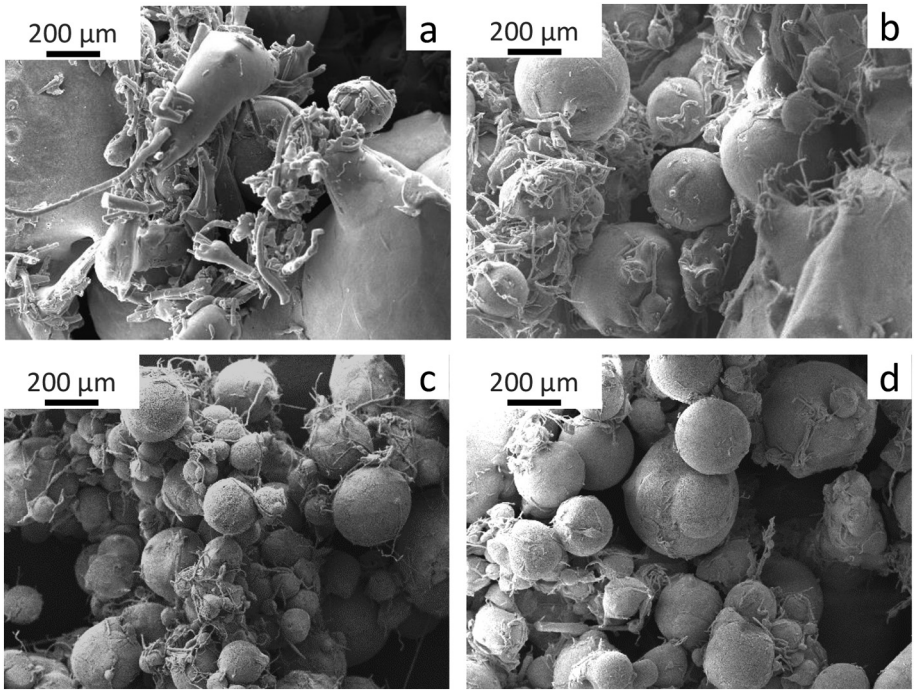

Fig. 4. SEM observations of freeze-granulated suspensions with various amounts of alumina and PEG-3 polymer. (a) 20 v.% alumina + 5 v.% PEG-3 (134 mPa.s), (b) 15 v.% alumina + 3,75 v.% PEG-3 (50 mPa.s), (c) 10 v.% alumina + 2,50 v.% PEG-3 (18 mPa.s) and (d) 15 v.% alumina + 2,2 v.% PEG-3 (20 mPa.s). Viscosity is taken at 100 s^{-1}.

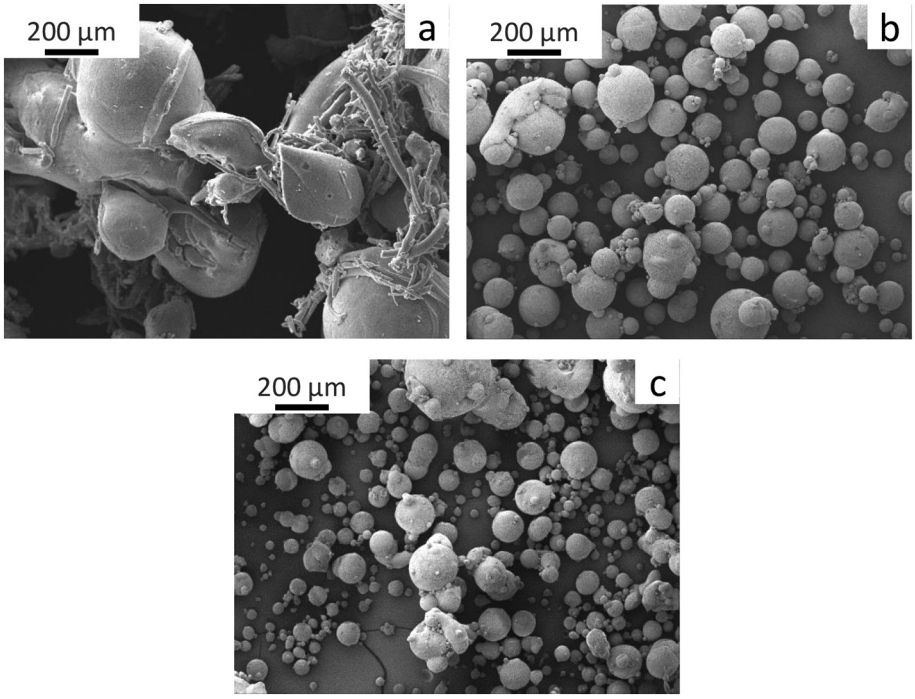

Fig. 5. SEM observations of freeze-granulated suspensions with 20 v.% alumina and 5 %v. of (a) PEG-3, (b) PEG-2 and (c) PEG-1 (molar mass decreases).

polymer are inadequate, the filament does not have time to resorb before impact with liquid nitrogen in this study, like with PEG-3.

3.3. Model of prediction of the granule size obtained by freeze granulation and spray drying

Laser granulometry is suitable to measure the granule size distribution, as shown in Fig. 6. In all the experiments done either by spray drying or freeze granulation, the size distribution is single-mode. Therefore the granule size of a batch is reduced to its d_{50} (median particle size in volume) in all the following results shown in this paper. We can also observe that in any case, for all the formulations, the granule size is always higher by freeze granulation than by spray drying. This is explained because the droplets are freezed very rapidly in the liquid nitrogen, and recovered through lyophilisation, leading to very small differences between the droplet size and the granule size. During spray drying, the droplets encounter a shrinkage because of the drying occurring in the hot chamber, and their final size is much smaller.

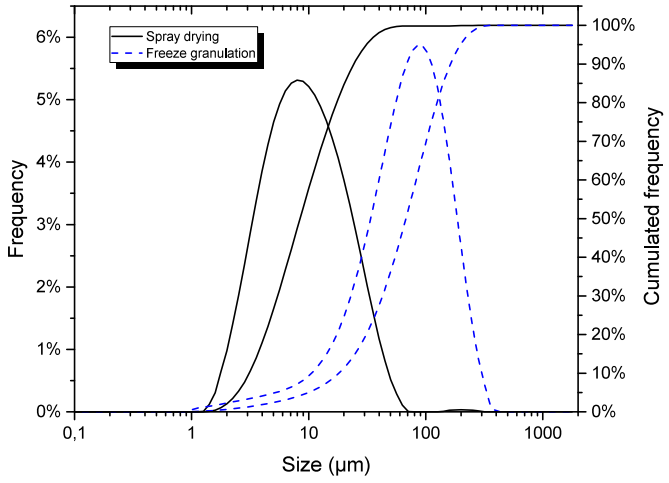

Fig. 6. Particle size distribution of granules made of alumina and PEOx-4 by spray drying and freeze granulation.

During the granulation process, the inlet liquid (suspension) is disrupted by a high velocity airflow to produce drops that can be disrupted themselves to produce smaller drops. Three stresses are considered for a liquid drop in a gas stream [32]:

- The spraying stress P_s, related to the relative velocity of the liquid with the gas (dynamic pressure) (Eq. 2).
- The stress related to the surface tension P_γ, related to the increase of the surface area, creating an opposing force to the fragmentation (Eq. 3).
- Under the spraying stress, drop is deformed. Due to the viscosity of the liquid drop, a viscous stress is created P_η (Eq. 4).

$$P_s \propto \rho_g u^2 \tag{2}$$

$$P_\gamma \propto \gamma_l / d \tag{3}$$

$$P_\eta \propto \frac{\eta_l}{d}\sqrt{\frac{P_s}{\rho_l}} \tag{4}$$

With ρ the density (kg/m^3), γ the surface tension (N/m), η the dynamic viscosity (Pa.s), u the relative velocity of air and liquid (m/s) and d the drop diameter (m). Subscripts g and l are related to the gas and liquid phase, respectively.

Thus, to promote the spraying, the spraying stress must be maximal (***process*** parameter), whereas viscosity and surface tension must be minimized (***formulation*** parameters). From these three stresses, one can build two dimensionless numbers Re* and We*, representing the competition between the disruptive spraying force and the viscosity (Eq. 5) and surface tension force (Eq. 6).

$$Re^* = \frac{P_s}{P_\eta} = \frac{d_n\sqrt{\rho_g \rho_l}u}{\eta_l} \tag{5}$$

$$We^* = \frac{P_s}{P_\gamma} = \frac{d_n \rho_g u^2}{\gamma_l} \quad (6)$$

Re* is similar to the Reynold number, considering the density of the two phases (gas and liquid). We* is similar to the Weber number, with the characteristics of the gas (ρ_g) and the liquid (γ_l). Surface tension and viscous stresses use the diameter of the drop as the characteristic length. However, in the case of spraying (Re* and We*), the diameter of the nozzle (d_n) is preferred. The higher Re* and We*, the higher the spraying stress, compared to the viscous and surface tension stresses respectively. Thus, the final droplet size is smaller with higher Re* and We*. From Re* and We*, a unique dimensionless number is created and called pulverization number Pu (Eq. 7).

$$Pu = \sqrt{Re^* \times We^*} = \frac{P_s}{\sqrt{P_\eta P_\gamma}} = \frac{d_n \rho_g{}^{3/4} \rho_l{}^{1/4} u^{3/2}}{\sqrt{\gamma_l \eta_l}} \quad (7)$$

This number represents the competition between the disruptive forces (from dynamic pressure) and the forces opposed to the deformation (from viscosity and surface tension).

Different suspensions were formulated with variable concentrations of alumina powder and organic additives at different concentrations. Their viscosity, surface tension and density were measured, and used to calculate the corresponding pulverization number Pu (see Table S2 in Supplementary Material). In addition, some suspensions were sprayed with higher air velocity u. The air velocity is estimated from the volume of air ejected in a given time and the diameter of the nozzle. Fig. 7 shows the variation of the mean size of granules produced by freeze-granulation with the pulverization number. This figure clearly proves that the granule size is only related to the pulverization number, and does not depend on the nature of the additive. The R^2_{aj} coefficient, related to the quality of the correlation, is equal to 88%. The constant coefficient of the model represents the effect of the process parameters, which are not taken into account in Pu, like feed rate of the suspension, the travel time of drops and so on.

The relationship between the mean granule size and Pu is valid over a wide range of size and Pu, granule size varying from 22 μm with RE, up to 420 μm with PEG-2 and PEG-3. Therefore, by using this new parameter, one can have a very high degree of prediction on the final size of the granules obtained by freeze-granulation, and thus a very robust and efficient method to adapt the parameters of the formulation and/or the process. Although the equation produces good results with the experimental data, Pu does not take into account several variables that can have an impact on the size of the granules: geometry of the nozzle (beyond its diameter), distance between the nozzle and the liquid nitrogen, pumping speed of the suspension. It is likely that other equipment would result in variations in the value of the coefficients, including the constant shown in Fig. 7.

This new parameter has to be adapted in the case of spray drying. In freeze granulation, the size of the droplets is close to size of the granules, because they are freezed very rapidly and recovered by sublimation. Whereas during the spray drying process, the droplets encounter a shrinkage because of the drying occurring in the hot chamber. Indeed Pu is related to the drop size, which is equal to the granule size in freeze granulation but not in spray drying. In addition, two different spray dryers were used in this study, which leads to a variation in numerous parameters: size of the drying chamber, velocity of the drying air, nozzle size, efficiency of the cyclone and so on. Consequently, the Pu parameter is splitted into two parts: the first one (Mat) is related to the material properties and the second one (Pro) is related to the equipment.

$$Mat = \frac{Pu}{\left(C^{vol}_{alumina} + C^{vol}_{add}\right) d_b u^{3/2}} = \frac{\rho_g{}^{3/4} \rho_l{}^{1/4}}{\left(C^{vol}_{alumina} + C^{vol}_{add}\right) \sqrt{\gamma_l \eta_l}} \quad (8)$$

$$Pro = \begin{cases} 1 \text{ with spray drier } SD1 \\ 2 \text{ with spray drier } SD2 \end{cases} \quad (9)$$

$$Pu' = Mat^{\beta_1} \times Pro^{\beta_2} \quad (10)$$

The process parameters in Pro are not explicit (Eq. 9), and β_1 and β_2 are two constants to be determined. Pu′ number is fitted to the data, the results are shown in Fig. 8 (see table S3 in Supplementary Material for the numerical values). R^2aj is 71%, which gives a relatively good agreement with the data, but not excellent. Actually, it is expected that the drying has a large impact on the granule size, and the granule shape (hollow spherical, full spherical, donut-like). Full spherical shape is favoured by a low inlet temperature, a low content and molar mass of polymer, a high ceramic loading, a high yield shear stress [9], and a high viscosity [33]. In addition to the granule shape, segregation of the polymer in solution may occur. Segregation is favoured by a high polymer content, a high liquid content, a large drop and a high evaporation rate [15]. Granule shape has a direct impact on their size,

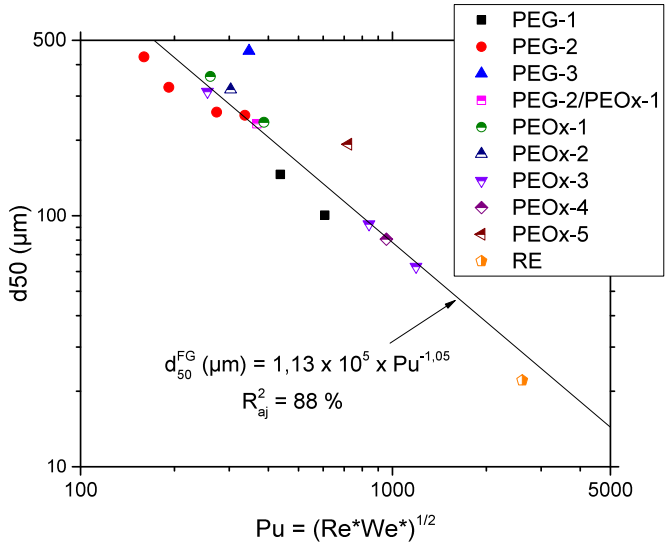

Fig. 7. Influence of the pulverization number on the mean granule size produced by freeze granulation.

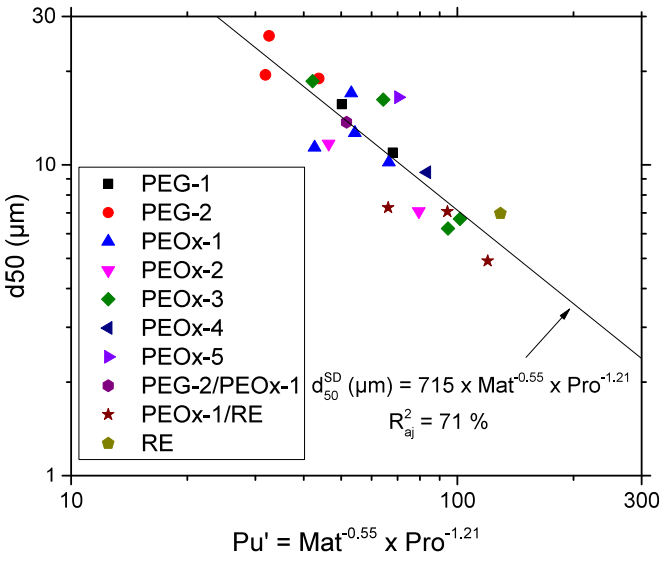

Fig. 8. Spray dried granule size as a function of the modified pulverization number Pu'.

which explains the lower quality of the fitting compared to the freeze granulation data with Pu.

3.4. Granule morphology

Fig. 9 compares the morphology of some granules obtained by freeze granulation and spray drying. Freeze-dried granules are mainly full and spherical whereas spray-dried ones have a greater variety of morphologies: one can find hollow are donut-like shapes as dense and full for a same product. That variability is in agreement with the difficulty to predict the spray-dried granule size without considering the drying as presented at Fig. 8. Freeze-dried granules are smoother and present a lower compacity. Indeed, the droplets do not shrink during the freeze-drying and the volume initially occupied by water becomes porosity.

Freeze granulation leads to typical morphologies with polymer-coated areas and others with apparent porosities (Fig. 10 a). Below a notched surface polymer films are no longer visible. Spray dried granule surface can be polymer-coated or not, depending on the formulation of the suspension (Fig. 10 b–c).

4. Conclusions

This comparative study of spray drying and freeze granulation was conducted for the preparation of mixed granules of submicronic alumina with a high content of polymeric binder. First, the variation of the viscosity of the ceramic suspensions filled with a high molecular weight polymer or with a dispersed rosin ester was studied. The polymer content has a very large impact on the viscosity but not on the flow index. In comparison, the use of rosin ester leads to very low viscosities, even at high dry matter contents.

Suspensions with varying viscosities (7–208 mPa.s), densities (1.31–1.76) and surface tensions (23–40 mN/m) were then granulated. The first observations reveal the importance of the content and the molar mass of the binder. It turns out that too high elasticity of the suspension leads to granulation failure. It is therefore essential to select an appropriate molar mass / additive concentration combination. Then by studying the forces involved, it was possible to propose a new and unified dimensionless number called pulverization number Pu to predict the size of the granules produced by freeze granulation from simple material (density, viscosity, surface tension) and process (velocity) data. This parameter is valid over a wide range of granule size (22 to 420 μm). Pu has been adjusted for spray drying, to partially take into account evaporative drying. However, the model is less effective in predicting granule size. Presumably, this difference is due to the fact that the constructed dimensionless number Pu is rather a predictor of droplet size and not of granule size. These two sizes are equal in the case of freeze granulation because the droplets are frozen and the water is removed without any shrinkage. On the contrary, by spray drying, the evaporation can lead to a significant shrinkage or not, depending on the morphology of the granule obtained. The amplitude of the

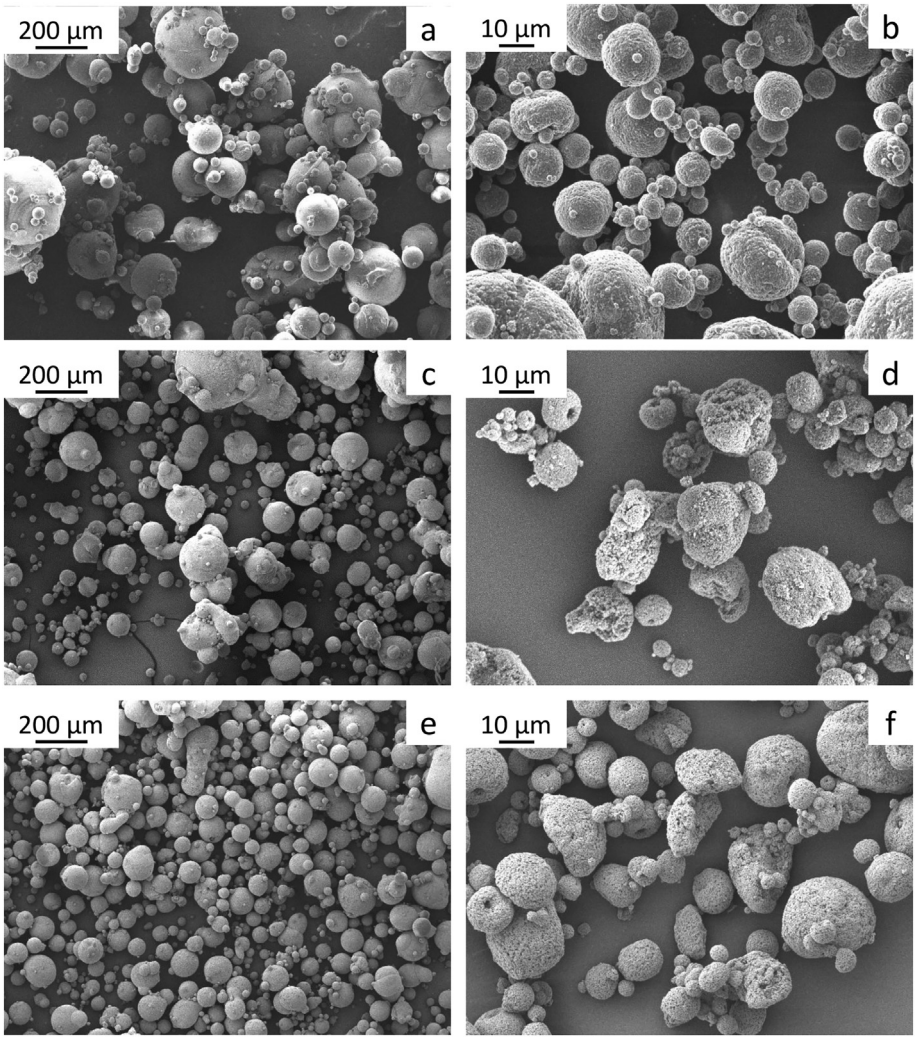

Fig. 9. SEM observations of (a,c,e) freeze dried and (b,d,f) spray-dried granules made of (a,b) 20 v.% PEOx-3, (c,d) 20 v.% PEG-1 and (e,f) 25 v.% PEG-1.

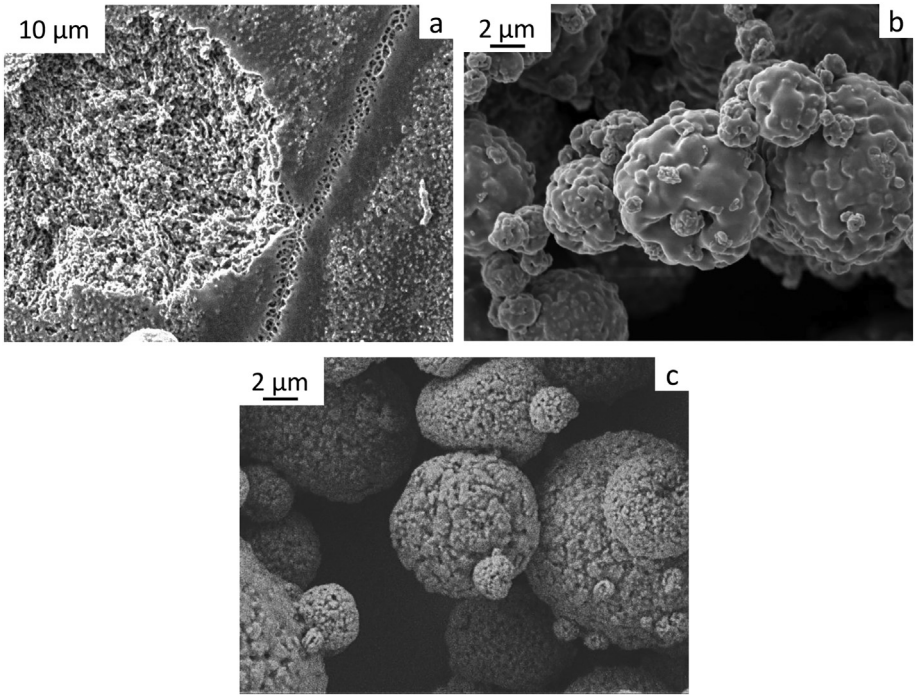

Fig. 10. SEM observations of (a) freeze-dried granule made of 20 v.% PEOx-3 and spray-dried granules made of (b) 50 v.% and (c) 20 v.% PEOx-5.

shrinkage has not been taken into account, which leads to a greater difficulty in predicting the size of the sprayed granules. To confirm this hypothesis, the drop size produced by atomization could be measured in a future study and compared to the prediction made using Pu. In addition, reproducibility tests will be needed to confirm the results presented in this article.

The freeze-dried granules are mostly full and spherical with high degree of porosity, which corresponds to the place occupied by the water before freeze-drying of the frozen droplet. The spray-dried granules are of various shapes, even for the same batch. The morphologies found are the dense spherical shape, the hollow shape and the donut shape.

Declaration of Competing Interest

The authors declare that they have no known competing financial interests or personal relationships that could have appeared to influence the work reported in this paper.

Acknowledgments

The authors would like to thank Safran Ceramics for the financial support (and in particular Gautier Mécuson) and Jérôme Kiennemann from Alteo (France) for the kindly supplying of alumina powder used in this research. We would also like to thank François Louvet, Associate Professor at the University of Limoges, for the technical expertise in construction the experimental matrices for the rheology study and for the subsequent data processing.

Appendix A. Supplementary data

Supplementary data to this article can be found online at https://doi.org/10.1016/j.powtec.2021.09.044.

References

[1] A. Sosnik, K.P. Seremeta, Advantages and challenges of the spray-drying technology for the production of pure drug particles and drug-loaded polymeric carriers, Adv. Colloid Interf. Sci. 223 (2015) 40–54.
[2] K. Subramanian, N. Vail, J. Barlow, H. Marcus, Selective laser sintering of alumina with polymer binders, Rapid Prototyp. J. 1 (1995) 24–35.
[3] J.C. Nelson, N.K. Vail, J. Barlow, J.J. Beaman, D.L. Bourell, H.L. Marcus, Selective laser sintering of polymer-coated silicon carbide powders, Ind. Eng. Chem. Res. 34 (1995) 1641–1651.
[4] N.K. Vail, J.W. Barlow, Effect of Polymer Coatings as Intermediate Binders on Sintering of Ceramic Parts, in, 1991.
[5] C. Lee, H. Choi, C. Lee, H. Kim, Photocatalytic properties of nano-structured TiO_2 plasma sprayed coating, Surf. Coat. Technol. 173 (2003) 192–200.
[6] E. Sanchez, E. Bannier, V. Cantavella, M.D. Salvador, E. Klyatskina, J. Morgiel, J. Grzonka, A.R. Boccaccini, Deposition of Al_2O_3-TiO_2 nanostructured powders by Atmospheric Plasma Spraying, J. Therm. Spray Technol. 17 (2008) 329–337.
[7] J.L. Amoros, V. Cantavella, J.C. Jarque, C. Feliu, Fracture properties of spray-dried powder compacts: effects of granule size, J. Eur. Ceram. Soc. 28 (2008) 2823–2834.
[8] J.-M. Haussonne, C. Carry, P. Bowen, J. Barton, Atomisation, Traité Des Matériaux. Céramiques et Verres : Principes et Techniques d'élaboration, Presses Polytechniques et Universitaires Romandes 2005, pp. 198–201.
[9] W.J. Walkers, J.S. Reed, Influence of Slurry parameters on the characteristics of Spray-Dried Granules, J. Am. Ceram. Soc. 82 (1999) 1711–1719.
[10] N.K. Vail, J.W. Barlow, Microencapsulation of Finely Divided Ceramic Powders, International Solid Freeform Fabrication Symposium, 1990.
[11] N. Vail, J.W. Barlow, Ceramic Structures by Selective Laser Sintering of Microencapsulated, Finely Divided Ceramic Materials, in, 1992.
[12] A. Stunda-Zujeva, Z. Irbe, L. Berzina-Cimdina, Controlling the morphology of ceramic and composite powders obtained via srapy drying - A review, Ceram. Int. 43 (2017) 11543–11551.
[13] P. Ramavath, R. Papitha, M. Ramesh, P.S. Babu, R. Johnson, Effect of primary particle size on spray formation, morphology and internal structure of alumina granules and elucidation of flowability and compaction behavior, Process. Appl. Ceram. 8 (2014) 93–99.
[14] S. Baklouti, T. Chartier, J.F. Baumard, Binder Distribution in Spray-Dried Alumina Agglomerates, J. Eur. Ceram. Soc. 18 (1998) 2117–2121.
[15] Y. Zhang, X. Tang, N. Uchida, K. Uematsu, Binder surface segregation during spray drying of ceramic slurry, J. Mater. Res. 13 (1998) 1881–1887.
[16] K. Rundgren, O. Lyckfeldt, M. Sjostedt, Improving Powders With Freeze Granulation, Ceram. Ind. 153 (2003) 40–44.
[17] S. Shanmugam, Granulation techniques and technologies: recent progresses, Bioimpacts 5 (2017) 55–63, https://doi.org/10.15171/bi.2015.04.
[18] M. Vicent, E. Sanchez, T. Molina, M.I. Nieto, R. Moreno, Comparison of freeze drying and spray drying to obtain porous nanostructured granules from nanosized suspensions, J. Eur. Ceram. Soc. 32 (2012) 1019–1028.
[19] B.P.C. Raghupathy, J.G.P. Binner, Spray Granulation of Nanometric Zirconia Particles, J. Am. Ceram. Soc. 94 (2011) 42–48.
[20] F. La Lumia, L. Ramond, C. Pagnoux, G. Bernard-Granger, Fabrication of homogenous pellets by freeze granulation of optimized TiO_2-Y_2O_3 suspensions, J. Eur. Ceram. Soc. 39 (2019) 2168–2178.
[21] M. Stuer, Z. Zhao, P. Bowen, Freeze granulation: Powder processing for transparent alumina applications, J. Eur. Ceram. Soc. 32 (2012) 2899–2908.

[22] G. Miao, W. Du, M. Moghadasi, Z. Pei, C. Ma, Ceramic binder jetting additive manufacturing: Effects of granulation on properties of feedstock powder and printed and sintered parts, Addit. Manuf. 36 (2020) 101542.
[23] W. Du, G. Miao, L. Liu, Z. Pei, C. Ma, Binder jetting additive manufacturing of ceramics feedstock powder preparation by spray freeze granulation, Proceedings of the AMSE 2019, 2019 , MSEC2019-3001.
[24] F. La Lumia, L. Ramond, C. Pagnoux, P. Coste, F. Lebreton, J.-R. Sevilla, G. Bernard-Granger, Dense and homogeneous MOX fuel pellets manufactured using the freeze granulation route, J. Am. Ceram. Soc. 103 (2020) 3020–3029.
[25] J. Ferguson, N. Hudsen, B. Warren, The break-up of fluids in an extensional flow field, J. Non-Newtonian Fluid Mech. 44 (1992) 37–54.
[26] S. Baklouti, J. Bouaziz, T. Chartier, J.F. Baumard, Binder burnout and evolution of the mechanical strength of dry-pressed ceramics containing poly(vinyl alcohol), J. Eur. Ceram. Soc. 21 (2001) 1087–1092.
[27] J. Cesarano, A. Aksay, A. Bleier, Stability of aqueous α-Al_2O_3 suspensions with poly (methacrylic acid) polyelectrolyte, J. Am. Ceram. Soc. 71 (1988) 250–255.
[28] M. Zhou, K. Huang, D. Yang, X. Qiu, Development and evaluation of polycarboxylic acid hyper-dispersant used to prepare high-concentrated coal–water slurry, Powder Technol. 229 (2012) 185–190.
[29] V.M. Entov, E.J. Hinch, Effect of a spectrum of relaxation times on the capillary thinning of a filament of elastic liquid, J. Non-Newtonian Fluid Mech. 72 (1997) 31–53.
[30] S.L. Anna, G.H. McKinley, Elasto-capillary thinning and breakup of model elastic liquids, J. Rheol. 45 (2001) 115–138.
[31] M.S. Oliveira, G.H. McKinley, Iterated stretching and multiple beads-on-a-string phenomena in dilute solutions of highly extensible flexible polymers, Phys. Fluids 17 (2005), 071704.
[32] J.O. Hinze, Fundamentals of the Hydrodynamic Mechanism of Splitting in Dispersion Processes, AICHE J. 1 (1955) 289–295.
[33] D.-J. Kim, J.-Y. Yung, Granule performance of irconia/alumina composite powders spray-dried using polyvinyl pyrrolidone binder, J. Eur. Ceram. Soc. 27 (2007) 3177–3182.